Since January 2020 Elsevier has created a COVID-19 resource centre with free information in English and Mandarin on the novel coronavirus COVID-19. The COVID-19 resource centre is hosted on Elsevier Connect, the company's public news and information website.

Reproductive Toxicology 114 (2022) 1–6

Contents lists available at ScienceDirect

Reproductive Toxicology

journal homepage: www.elsevier.com/locate/reprotox

Reproductive toxicity of ritonavir in male: Insight into mouse sperm capacitation

Eun-Ju Jung, Woo-Jin Lee, Ju-Mi Hwang, Jeong-Won Bae, Woo-Sung Kwon *

Department of Animal Science and Biotechnology, Kyungpook National University, Sangju, Gyeongsangbuk-do 37224,Republic of Korea

ARTICLE INFO

Handling Editor: Anna Price

Keywords:
Ritonavir
Spermatozoa
Capacitation
AKT pathway
Male fertility

ABSTRACT

Since COVID-19 began in 2019, therapeutic agents are being developed for its treatment. Among the numerous potential therapeutic agents, ritonavir (RTV), an anti-viral agent, has recently been identified as an important element of the COVID-19 treatment. Moreover, RTV has also been applied in the drug repurposing of cancer cells. However, previous studies have shown that RTV has toxic effects on various cell types. In addition, RTV regulates AKT phosphorylation within cancer cells, and AKT is known to control sperm functions (motility, capacitation, and so on). Although deleterious effects of RTV have been reported, it is not known whether RTV has male reproduction toxicity. Therefore, in this study, we aimed to investigate the effects of RTV on sperm function and male fertility. In the present study, sperm collected from the cauda epididymis of mice were incubated with various concentrations of RTV (0, 0.1, 1, 10, and 100 μM). The expression levels of AKT, phospho-AKT (Thr^{308} and Ser^{473}), and phospho-tyrosine proteins, sperm motility, motion kinematics, capacitation status, and cell viability were assessed after capacitation. The results revealed that AKT phosphorylation at Thr^{308} and Ser^{473} was significantly increased, and the levels of tyrosine-phosphorylated proteins (at approximately 25 and 100 kDa) were significantly increased in a dose-dependent manner. In addition, RTV adversely affected sperm motility, motion kinematics, and cell viability. Taken together, RTV may have negative effects on sperm function through an abnormal increase in tyrosine phosphorylation and phospho-AKT levels. Therefore, individuals taking or prescribing RTV should be aware of its reproductive toxicity.

1. Introduction

Since the COVID-19 pandemic in 2019, researchers have been developing a treatment [1–3]. Among the various candidate chemical compounds, ritonavir (RTV), a protease inhibitor (PI), has been effective in treating COVID-19. RTV is a well-known therapeutic chemical for acquired immune deficiency syndrome (AIDS) [4] and is widely used to treat various viral infections. Moreover, several studies have recently reported that RTV can be used to treat cancer [5–7]. Several studies have shown that RTV affects various types of cancer cells by reducing the phosphorylation of protein kinase B (AKT) [6,8,9]. RTV inhibits the AKT pathway in a dose-dependent manner in pancreatic ductal adenocarcinoma cell lines [6], with a stable total AKT level; however, in another study, phospho-AKT (Ser^{473}) level decreased and apoptosis was induced in breast cancer cells [8]. Moreover, RTV exhibits synergistic effect when treated with AKT siRNA, leading to apoptosis in ovarian cancer cells [9].

Although RTV can be used in anti-viral and anti-cancer treatment regimens, several studies have reported that RTV can affect abnormal functions in normal cells [10,11]. RTV exerts cytotoxicity and ER stress in Hepa RG cell lines in a concentration-dependent manner [10]. In addition, RTV affects cell viability, LDH release, mitochondrial DNA damage, and apoptosis in human dermal microvascular endothelial cells [11]. However, reproductive toxicity of RTV has not been reported.

Ejaculated sperm cells undergo maturation, called 'capacitation,' to facilitate sperm-egg fusion [12,13]. During capacitation, tyrosine phosphorylation occurs, and only capacitated spermatozoa undergo the acrosome reaction [14]. AKT plays an important role in spermatozoa and is related to sperm function during capacitation. It has been reported that motility, hyperactivation, acrosome reaction, and tyrosine phosphorylation are associated with AKT during capacitation [15,16]. Although RTV can be used for cancer treatment, the toxicity of RTV has also been emphasized in studies on various cell types [10,11]. RTV could also exert reproductive toxicity because AKT plays an important role in sperm function and male fertility. However, there is no research on the toxicity of AKT-related RTV on sperm function and male fertility.

* Corresponding author.
E-mail address: wskwon@knu.ac.kr (W.-S. Kwon).

https://doi.org/10.1016/j.reprotox.2022.09.008
Received 25 May 2022; Received in revised form 14 September 2022; Accepted 30 September 2022
Available online 2 October 2022

Therefore, the present study was designed to investigate the effects of RTV on sperm function following AKT regulation in spermatozoa during capacitation.

2. Materials and methods

All procedures were conducted according to the guidelines for the ethical treatment of animals and approved by the Institutional Animal Care and Use Committee of Kyungpook National University.

2.1. Media and chemicals

All the reagents were purchased from Sigma-Aldrich (St. Louis, MO, USA). Modified Tyrode's medium was used as the basic medium (BM) (97.84, mM NaCl; 1.42 mM, KCl; 0.47 mM, $MgCl_2{\cdot}6H_2O$; 0.36 mM, $NaH_2PO_4{\cdot}H_2O$; 5.56 mM, D-glucose; 25 mM, $NaHCO_3$; 1.78 mM, $CaCl_20.2\ H_2O$; 24.9 mM, Na-lactate; 0.47 mM, Na-pyruvate; 50 μg/mL, gentamycin; and 0.005 mM, phenol red). Bovine serum albumin (0.4 %) was added to BM to induce capacitation [17,18].

2.2. Preparation and treatment of spermatozoa

ICR mice were bred at 22 ± 2 °C with proper humidity under 12 h light/dark cycle. All mice were supplied with food (Cargill Agripurina Inc., Korea) and water ad libitum. 3 mice were utilized per experiment as previously described [19]. Mature male mice aged 8–12 weeks were sacrificed by cervical dislocation, and the cauda epididymis was extracted. Finally, the spermatozoa were collected by puncturing the epididymis using a sterile needle. The spermatozoa were incubated with different concentrations of RTV (0, 0.1, 1, 10, and 100 μM) under 5 % CO_2 and 37 °C for 90 min to induce capacitation [17]. The concentration range of RTV was based on previous studies [9,20,21].

2.3. Western blotting of AKT, phospho-AKT (Thr^{308} and Ser^{473}), and tyrosine phosphorylation

Levels of AKT, phospho-AKT (Thr^{308} and Ser^{473}), and tyrosine phosphorylation were measured using western blotting. Each sample was washed twice with Dulbecco's phosphate-buffered saline (DPBS). The samples were resuspended in modified Laemmli sample buffer (315 mM Tris, 10 % glycerol, 10 % SDS, 5 % 2-mercaptoethanol, and 5 % bromophenol blue) and incubated at room temperature (RT) for 10 min. Then, the samples were centrifuged at 10,000 × *g* for 5 min, and the supernatants were boiled at 95 °C for 3 min. The protein samples were separated via 12 % SDS-PAGE (MiniPROTEIN Tetra Cell, Bio-Rad, Hercules, CA, USA) and then transferred to PVDF membranes (Bio-Rad, Hercules, CA, USA). The membranes were incubated with 3 % ECL blocking agent (GE Healthcare, Chicago, IL, USA) for 2 h at RT. After washing the membranes with DPBS containing 0.1 % Tween 20 (PBS-T), the membranes were incubated with primary antibodies. The primary antibodies were diluted with 3 % ECL blocking agent [Anti-alpha Tubulin antibody [DM1A] (Abcam, Cambridge, UK), 1:5000; anti-AKT antibody (Cell Signaling Technology, Danvers, Massachusetts, USA), 1:1000; anti-phospho-AKT (Thr^{308}) antibody (Cell Signaling Technology, Danvers, Massachusetts, USA), 1:1000; anti-phospho-AKT (Ser^{473}) antibody (Genetex, Inc, Irvine, CA, USA), 1:1000; anti-phosphotyrosine antibody [PY20] (HRP) (Abcam, Cambridge, UK), 1:5000]. After the membranes were incubated with each antibody, they were washed with PBS-T. Goat anti-mouse IgG H&L (HRP) (Abcam, Cambridge, UK) and goat anti-rabbit IgG H&L (HRP) (Cell Signaling Technology, Danvers, Massachusetts, USA) were diluted at 1:2000 with 3 % ECL blocking agent and used as secondary antibodies. Proteins were detected using the iBright™ CL1500 Imaging System (ThermoFisher Scientific, Waltham, MA, USA) by the enhanced chemiluminescence method. The Image Studio Lite (Version 5.2, LI-COR Corporate, Lincoln, NE, USA) system was used to analyze the protein expression levels. The density ratio of each treatment band was normalized to that of α-tubulin.

2.4. Sperm motility and motion kinematics

Sperm motility and motion kinematics were analyzed using a computer-assisted sperm analysis program (CASA) (FSA 2016, Medical Supply, Seoul, Korea). Sperm motility [total sperm motility (MOT, %), rapid sperm motility (RPD, %), medium sperm motility (MED, %), slow sperm motility (SLW, %), and progressive sperm motility (PRG, %)], motion kinematics [curvilinear velocity (VCL, μm/s), straight-line velocity (VSL, μm/s), average path velocity (VAP, μm/s), linearity (LIN, %), straightness (STR, %), beat–cross frequency (BCF, Hz), mean angular displacement (MAD, degree), wobble (WOB, %), dance (DNC, $\mu m^2/s$), mean dance (DNM, μm), and amplitude of lateral head displacement (ALH, μm)] were measured. Briefly, 10 μL of the treated sample was laid on a Makler counting chamber (Sefi-Medical Instruments, Haifa, Israel), which was placed on a 37 °C heating plate. More than five random fields were recorded. Finally, the images were analyzed using the FSA 2016 program.

2.5. Sperm capacitation status

In the present study, we used the dual staining method (combined Hoechst 33258/chlortetracycline fluorescence assessment) to evaluate the capacitation status [22]. The samples were centrifuged at 100 × *g* for 2.5 min. The supernatant (135 μL) was discarded, Hoechst 33258 (H33258) solution was added, and the samples were incubated for 2 min at RT. Then, 250 μL of 2 % (w/v) polyvinylpyrrolidone in DPBS was added, and the samples were centrifuged at 100 × *g* for 2.5 min. All supernatants were removed, and 100 μL of DPBS and chlortetracycline fluorescence (CTC) solution (750 mM CTC, 20 mM Tris, 130 mM NaCl, and 5 mM cysteine, pH 7.4) were added. Finally, capacitation status was observed using an OLYMPUS BX43 (Olympus, Tokyo, Japan) with fluorescence illumination, using ultraviolet BP340–380/LP425 and BP450–490/LP515 excitation/emission filters for H33258 and chlortetracycline fluorescence, respectively. At least 400 spermatozoa per slide were sorted into four patterns according to the capacitation status: dead (D pattern, blue fluorescence spread evenly on the sperm head), live non-capacitated (F pattern, bright green fluorescence spread evenly on the sperm head), live capacitated (B pattern, bright green fluorescence spread over the acrosomal region and a dark post-acrosomal region), and live acrosome reacted (AR pattern, no fluorescence over the sperm head or bright green fluorescence only in the post acrosomal region) [22].

2.6. Assessment of cell viability

Cell viability was evaluated using a Cell Cytotoxicity Assay Kit (Abcam, Cambridge, UK). The assay solution was added to a 96-well plate containing each sample. The samples were incubated at 37 °C in the dark for 3 h. After incubation, absorbance was measured at 570 and 650 nm (Gemini Em; Molecular Devices Corporation, Sunnyvale, CA, USA). Cell viability was assessed as the ratio of OD 570 nm to OD 650 nm (SoftMax Pro 7; Molecular Devices Corporation, Sunnyvale, CA, USA).

2.7. Statistical analysis

Data were analyzed using one-way ANOVA with the SPSS software (version 26.0, IBM, Armonk, NY, USA). Tukey's multiple comparison test was used to compare the four RTV-treated groups with the control group. Each experiment was conducted at least three times. Differences were considered significant when the p-value was less than 0.05 ($P < 0.05$). The data are expressed as the mean ± SEM.

3. Results

3.1. Expression levels of AKT, phospho-AKT (Thr^{308} and Ser^{473}), and tyrosine-phosphorylated proteins

The expression levels of AKT, phospho-AKT (Thr^{308} and Ser^{473}), and tyrosine-phosphorylated proteins were analyzed using western blotting. AKT and Thr^{308} were detected at approximately 60 kDa, and Ser^{473} was detected at approximately 56 kDa (Fig. 1D). Phospho-AKT (Thr^{308} and Ser^{473}) showed increasing patterns in dose-dependent manners. The level of Thr^{308} was significantly increased at 1 μM RTV concentration, and the level of Ser^{473} was significantly increased at highest RTV concentration (100 μM) ($P < 0.05$, Fig. 1B and C). In contrast, there was no significant difference in AKT levels ($P < 0.05$, Fig. 1A). These results indicate that the treatment of RTV on sperm increased the expression levels of phospho-AKT but not AKT. Phosphotyrosine substrates were detected at approximately 25 kDa, 60 kDa, and 100 kDa (Fig. 2B). The levels of phosphotyrosine substrates at approximately 25 and 100 kDa were significantly increased, whereas those at approximately 60 kDa were not significantly different ($P < 0.05$, Fig. 2). This indicates that the RTV significantly altered the tyrosine phosphorylation during the capacitation.

3.2. Effects of RTV on sperm motility and motion kinematics

MOT, RPD, PRG, VCL, BCF, DNC, and ALH were significantly decreased in all RTV treatment groups compared to those of the control group, whereas STR was significantly increased at highest concentration (100 μM) ($P < 0.05$, Table 1). In addition, WOB was significantly increased, whereas DNM was significantly decreased at high concentrations (10 and 100 μM) ($P < 0.05$, Table 1). The other parameters (MED, SLW, VSL, VAP, LIN, and MAD) did not significantly alter. This result indicates that treatment of RTV suppressed the sperm motility and motion kinematic parameters during the capacitation.

3.3. Effects of RTV on capacitation status and cell viability

The ratio of the AR pattern was significantly increased at high concentrations (10 and 100 μM), whereas the ratio of the B pattern was significantly decreased at highest RTV concentration (100 μM) compared to that of the control group ($P < 0.05$, Fig. 3A and B). There was no significant change in the proportion of the F pattern ($P < 0.05$, Fig. 3C). The ratio of cell viability significantly decreased at high concentrations (10 and 100 μM) ($P < 0.05$, Fig. 3D). These results mean that treatment of RTV increased acrosome reaction but decreased the capacitation abnormally.

4. Discussion

RTV is a PI that prevents viral replication by binding to the viral protease and was originally used for managing AIDS [4]. RTV is mainly used as a boosting agent because it can disrupt the metabolism of another PI. Thus, RTV has been used to assist various anti-viral agents [23]. Using this mechanism for COVID-19 treatments, RTV has been used for related research and has recently been adopted as a component of medicine [24]. In addition, RTV is listed in the WHO Model List of Essential Medicines, which lists drugs that are considered safe and effective to meet the most important requirements of the health system [25]. However, previous studies have shown that RTV is toxic to several cells [10,11]. Nevertheless, the toxicity of RTV to spermatozoa remains unknown.

AKT signaling is involved in cell survival, growth, and proliferation in cancer and normal cells [26]. In spermatozoa, AKT also regulates sperm function during capacitation [15,16]. AKT should be phosphorylated at Thr^{308} and Ser^{473} for its activation [27]. RTV regulates cancer cells by suppressing AKT phosphorylation [6,8,9]. However, there have been no studies on how RTV affects AKT phosphorylation in spermatozoa and its effects on sperm function. Therefore, this study was designed to investigate the changes in AKT phosphorylation caused by RTV and its effects on sperm function and male fertility.

In the present study, AKT and phosphorylated AKT (Thr^{308} and Ser^{473}) levels were measured to investigate how RTV affects AKT phosphorylation in spermatozoa. Interestingly, contrary to previous studies [6,8,9], our result showed that RTV treatment did not decrease the phosphorylation of Thr^{308} and Ser^{473}; however, the phosphorylation increased significantly compared to that of the control group in mouse

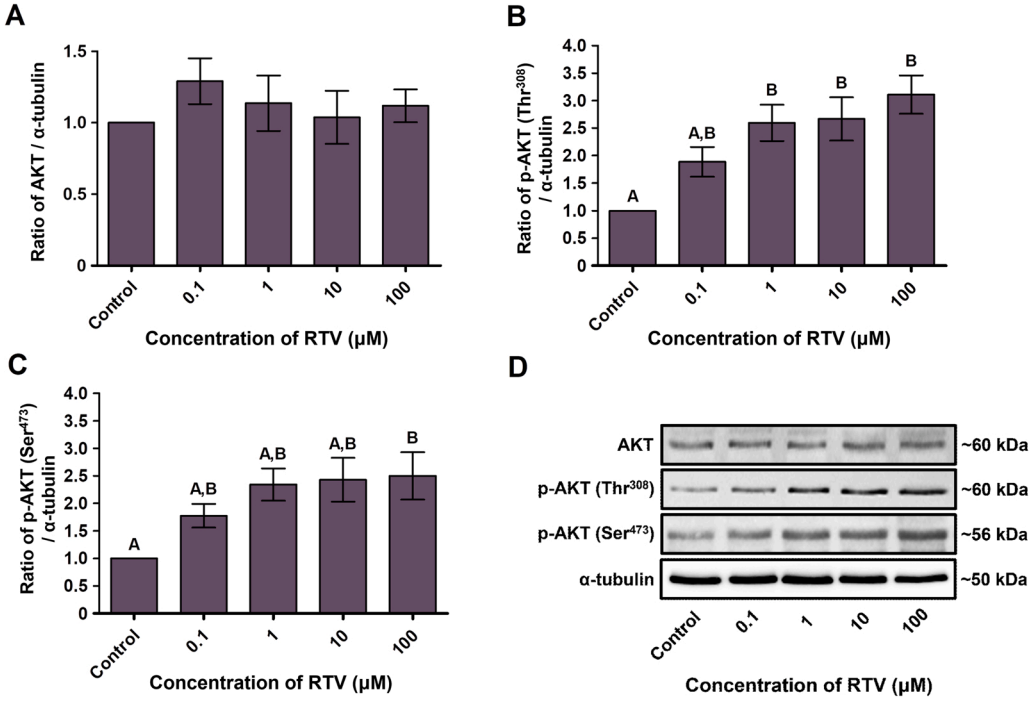

Fig. 1. Effects of ritonavir (RTV) on AKT and phosphorylated AKT (Thr^{308} and Ser^{473}) levels. (A) AKT level was measured at approximately 60 kDa. (B) Phosphorylated AKT (Thr^{308}) level was measured at approximately 60 kDa. (C) Phosphorylated AKT (Ser^{473}) level was measured at approximately 56 kDa. (D) AKT and phosphorylated AKT (Thr^{308} and Ser^{473}) were probed. Lane 1: Control; Lane 2: 0.1 μM RTV; Lane 3: 1 μM RTV; Lane 4: 10 μM RTV; Lane 5: 100 μM RTV. Data were evaluated by one-way ANOVA and expressed as mean ± SEM; n = 3. Values with different superscripts ($^{a, b, and c}$) indicate significant differences between the control and treatment groups ($P < 0.05$).

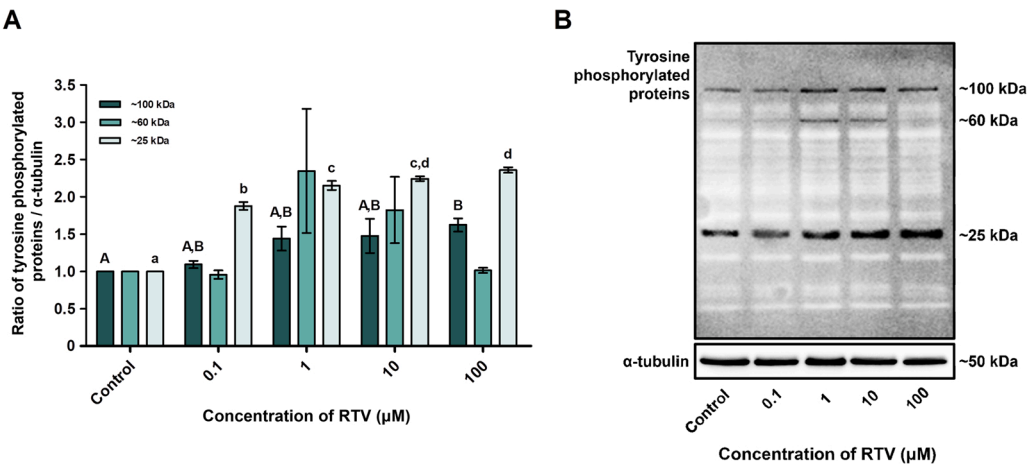

Fig. 2. Effect of ritonavir (RTV) on protein tyrosine phosphorylation. (A) The level of tyrosine phosphorylated proteins was measured at approximately 100, 60, and 25 kDa. (B) Tyrosine phosphorylated proteins were probed. Lane 1: Control; Lane 2: 0.1 μM RTV; Lane 3: 1 μM RTV; Lane 4: 10 μM RTV; Lane 5: 100 μM RTV. Data were evaluated by one-way ANOVA and expressed as mean ± SEM, n = 3. Values with different superscripts ($^{A, B, a, b, c, and d}$) indicate significant differences between the control and treatment groups ($P < 0.05$).

Table 1
Effects of Ritonavir (RTV) on sperm motility and motion kinematics.

Concentration of RTV (μM)					
	Control	0.1	1	10	100
MOT (%)	74.34 ± 0.76^{a}	67.31 ± 0.26^{b}	68.66 ± 0.51^{b}	67.91 ± 0.65^{b}	67.78 ± 1.70^{b}
RPD (%)	53.87 ± 0.05^{a}	48.81 ± 0.55^{b}	46.30 ± 0.26^{b}	47.03 ± 0.04^{b}	46.18 ± 1.32^{b}
MED (%)	14.54 ± 1.12	11.31 ± 0.32	15.44 ± 0.34	13.97 ± 1.23	12.91 ± 0.37
SLW (%)	4.94 ± 0.05	5.54 ± 0.17	6.94 ± 0.59	7.92 ± 0.07	6.91 ± 1.24
PRG (%)	68.40 ± 1.17^{a}	60.12 ± 0.87^{b}	61.72 ± 0.08^{b}	60.99 ± 1.19^{b}	60.69 ± 0.55^{b}
VCL (μm/s)	85.40 ± 1.37^{a}	76.46 ± 0.05^{b}	74.72 ± 0.81^{b}	71.22 ± 2.05^{b}	74.14 ± 0.85^{b}
VSL (μm/s)	28.78 ± 0.27	30.85 ± 1.04	31.10 ± 3.36	30.26 ± 0.46	33.56 ± 0.11
VAP (μm/s)	41.45 ± 2.37	42.86 ± 0.95	42.14 ± 3.25	41.42 ± 0.07	42.06 ± 2.14
LIN (%)	25.62 ± 0.92	26.74 ± 1.24	26.77 ± 0.63	29.80 ± 1.99	30.29 ± 1.41
STR (%)	64.61 ± 0.24^{a}	71.42 ± 058^{b,c}	69.69 ± 1.22^{b}	72.43 ± 0.98^{b,c}	74.88 ± 0.05^{c}
BCF (Hz)	6.31 ± 0.10^{a}	5.64 ± 0.02^{b}	5.26 ± 0.03^{c}	5.13 ± 0.06^{c}	5.30 ± 0.05^{c}
MAD (degree)	40.64 ± 0.16	40.45 ± 0.24	35.73 ± 1.12	37.36 ± 0.04	38.18 ± 2.24
WOB (%)	52.12 ± 0.80^{a}	56.19 ± 1.12^{a,b}	55.06 ± 1.29^{a,b}	58.11 ± 1.77^{b}	60.49 ± 0.87^{b}
DNC (μm^2/s)	300.09 ± 9.37^{a}	233.44 ± 1.85^{b}	203.86 ± 14.57^{b}	199.45 ± 10.94^{b}	212.74 ± 5.84^{b}
DNM (μm)	13.92 ± 0.68^{a}	11.38 ± 0.49^{a,b}	10.86 ± 0.89^{a,b}	9.69 ± 0.89^{b}	9.48 ± 0.61^{b}
ALH (μm)	3.42 ± 0.05^{a}	2.93 ± 0.01^{b}	2.76 ± 0.10^{b}	2.75 ± 0.08^{b}	2.75 ± 0.04^{b}

Sperm motility and motion kinematics are presented as the mean ± SEM; n = 3. MOT, sperm motility (%); RPD, rapid sperm motility (%); MED, medium sperm motility (%); SLW, slow sperm motility (%); PRG, progressive sperm motility (%); VCL, curvilinear velocity (μm/s); VSL, straight-line velocity (μm/s); VAP, average path velocity (μm/s); LIN, linearity (%); STR, straightness (%); BCF, beat cross frequency (Hz); MAD, mean angular displacement (degree); WOB, wobble (%); DNC, sperm dance (μm^2/s); DNM, sperm mean dance (μm); ALH, mean amplitude of lateral head displacement (μm). Values with different superscript characters ($^{a, b, and c}$) within the same row indicate significant differences ($P < 0.05$), as determined by one-way ANOVA.

spermatozoa (Fig. 1). Based on this result, we expect that RTV may affect abnormal AKT phosphorylation in spermatozoa through different signaling methods compared to that of other cells. Meanwhile, AKT phosphorylation is known to prevent sperm from DNA damage, oxidative stress, and spontaneous apoptosis during capacitation [28]. In addition, AKT phosphorylation at Thr^{308} and Ser^{473} by activated PI3 kinase was described to cause spontaneous acrosome reaction and prevent premature hyperactivation [16,29]. Similar to our results, recent study has reported that HA15 which inhibits glucose-regulated protein 78 (GRP78) abnormally increased the AKT level with alteration of AKT signaling pathway-related proteins (PI3K, p-PI3K, PTEN, p-PTEN, PDK1, and p-PDK1) in spermatozoa [30]. Therefore, it is anticipated that the alterations of AKT phosphorylation may be happened by AKT signaling pathway-related proteins in the present study. However, it is considered that further research is needed to clarify the alteration of AKT phosphorylation by RTV in our results.

Ejaculated spermatozoa undergo a special process called capacitation, which occurs in the female genital tract and enables spermatozoa to acquire the ability to fertilize. Tyrosine phosphorylation is caused by enzymes that are activated during capacitation. Finally, the sperm motility and motion kinematics are altered by the tyrosine phosphorylation [12,13]. In this study, the levels of tyrosine-phosphorylated proteins were measured. The results showed that the treatment of RTV significantly increased tyrosine phosphorylation (Fig. 2). In addition to tyrosine phosphorylation, AKT regulates sperm motility and kinematics. When AKT phosphorylation was inhibited by the AKT inhibitor SH-5, sperm motility, VCL, VSL, and VAP were significantly decreased in stallion spermatozoa [31]. Another AKT inhibitor Akti-2 suppressed total and progressive motility in mouse spermatozoa [15]. In this study, sperm motility and motion kinematic parameters were evaluated using the CASA system. RTV treatment significantly reduced MOT, RPD, and PRG, and suppressed VCL, BCF, DNC, DNM, and ALH (Table 1), despite increased AKT phosphorylation (Thr^{308} and Ser^{473}) (Fig. 1) and tyrosine phosphorylation (Fig. 2) during capacitation. These results indicate that exposure to RTV has adverse effects on sperm motility and motion kinematics during capacitation, and we suggest that this may be due to an abnormal increase in AKT phosphorylation and tyrosine phosphorylation.

Spermatozoa undergo the acrosome reaction after capacitation. The acrosome reaction is essential because only acrosome-reacted sperm can penetrate the zona pellucida and fuse with the oocyte [13]. In addition, the AKT signaling pathway is also involved in capacitation and the acrosome reaction [15,32]. Akti-2 inhibits the acrosome reaction in mouse spermatozoa induced by the calcium ionophore A23187 [15]. In

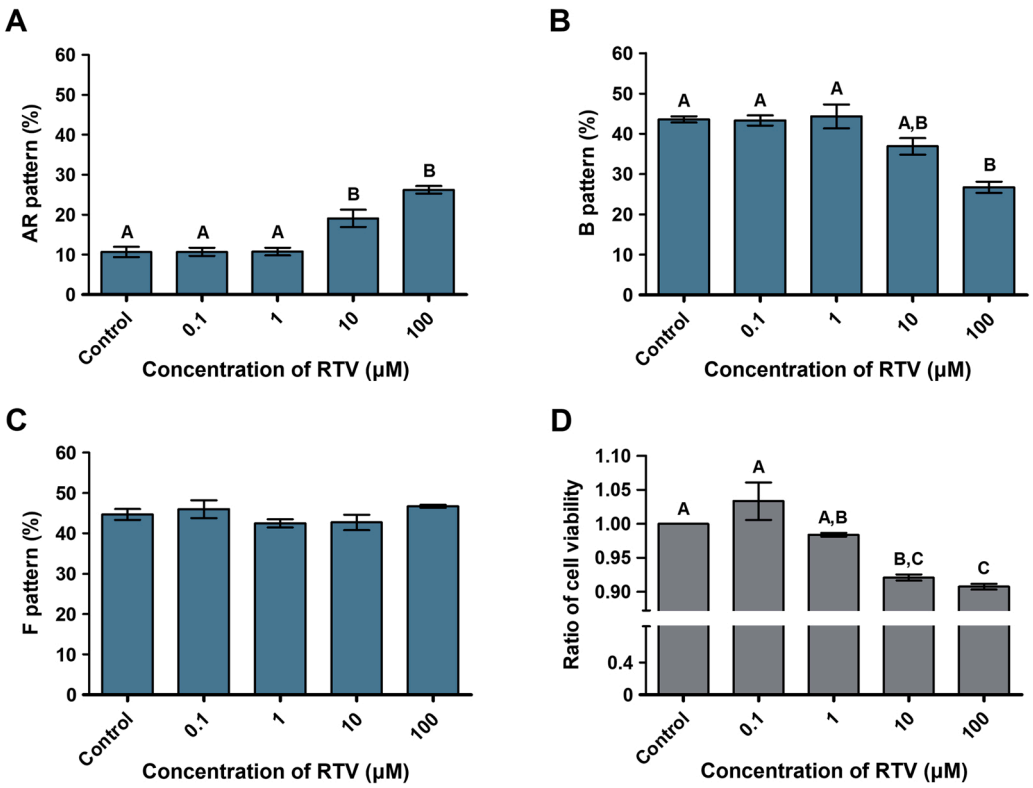

Fig. 3. Effects of ritonavir (RTV) on capacitation status and cell viability. (A) Live acrosome reacted pattern (AR pattern). (B) Live capacitated pattern (B pattern). (C) Live non-capacitated pattern (F pattern). (D) Cell viability levels after treatment with various RTV concentrations. Values with different superscripts ([a, b, and c]) indicate significant differences between the control and treatment groups ($P < 0.05$). Data were evaluated by one-way ANOVA and represent means ± SEM; n = 3.

addition, in the ZP3/ZP_{se}-induced acrosome reaction, ZP3/ZP_{se} stimulation increased AKT activation; moreover, when the sperm were treated with an AKT antagonist, PI3 kinase-dependent acrosome reaction decreased significantly in mouse spermatozoa [32]. Our results showed that RTV caused an increase in the ratio of acrosome-reacted spermatozoa (Fig. 3A), while the ratio of live-capacitated spermatozoa decreased (Fig. 3B), indicating that an abnormal acrosome reaction occurred after RTV treatment. Based on these results, we hypothesized that an abnormal increase in AKT phosphorylation and tyrosine phosphorylation also detrimentally affects sperm capacitation status. However, it is still unknown whether the change in tyrosine phosphorylation levels was due to AKT phosphorylation by RTV or whether RTV directly influenced tyrosine phosphorylation. According to previous research, AKT regulates tyrosine phosphorylation in spermatozoa. When AKT phosphorylation is disturbed, tyrosine phosphorylation level decreases in mouse spermatozoa [15]. Moreover, the recent study conducted in boar sperm showed that inhibition of GRP78 increased the AKT level with increased phospho-tyrosine levels [30]. Our results also showed that RTV treatment increased both the AKT phosphorylation and tyrosine phosphorylation. Therefore, we assume that there may be an interaction between AKT phosphorylation and tyrosine phosphorylation. However, direct evaluation is needed to determine the exact signal transduction system between AKT and tyrosine phosphorylation in spermatozoa.

RTV is known to have adverse effects on the viability of various cell types [11,33]. Similar to these results, RTV treatment suppressed cell viability in mouse spermatozoa in the present study (Fig. 3D). It has also been reported that phosphorylated AKT is important for stallion spermatozoa [31]. Thus, the decrease in cell viability observed in this study might be related to abnormally increased AKT phosphorylation.

5. Conclusion

RTV is one of the anti-viral agents currently used for COVID-19 treatment; it is also used for anti-cancer-related research involving inhibition of AKT phosphorylation. Our results showed that RTV abnormally increased AKT and tyrosine phosphorylation and suppressed sperm funtions during capacitation. Therefore, we suggest that special attention is required when prescribing this drug and the patients must be warned about its reproductive toxicity. In addition, the present study is the first to elucidate the reproductive toxicity of RTV in association with AKT. Thus, we anticipate that the present study will provide useful data for further reproductive toxicity studies.

Declaration of Competing Interest

The authors declare that they have no known competing financial interests or personal relationships that could have appeared to influence the work reported in this paper.

References

[1] M.A. Martinez, Compounds with therapeutic potential against novel respiratory 2019 coronavirus, Antimicrob. Agents Chemother. 64 (5) (2020) e00399-20.
[2] L.R. Baden, E.J. Rubin, Covid-19—the search for effective therapy, New Engl. J. Med. 382 (19) (2020) 1851–1852.
[3] M. Wang, R. Cao, L. Zhang, X. Yang, J. Liu, M. Xu, Z. Shi, Z. Hu, W. Zhong, G. Xiao, Remdesivir and chloroquine effectively inhibit the recently emerged novel coronavirus (2019-nCoV) in vitro, Cell Res. 30 (3) (2020) 269–271.
[4] D.J. Kempf, K.C. Marsh, J.F. Denissen, E. McDonald, S. Vasavanonda, C.A. Flentge, B.E. Green, L. Fino, C.H. Park, X.-P. Kong, ABT-538 is a potent inhibitor of human immunodeficiency virus protease and has high oral bioavailability in humans, Proc. Natl. Acad. Sci. 92 (7) (1995) 2484–2488.
[5] M.W.-H. Wang, S. Wei, R. Faccio, S. Takeshita, P. Tebas, W.G. Powderly, S. L. Teitelbaum, F.P. Ross, The HIV protease inhibitor ritonavir blocks osteoclastogenesis and function by impairing RANKL-induced signaling, J. Clin. Investig. 114 (2) (2004) 206–213.

[6] R.B. Batchu, O.V. Gruzdyn, C.S. Bryant, A.M. Qazi, S. Kumar, S. Chamala, S. T. Kung, R.S. Sanka, U.S. Puttagunta, D.W. Weaver, S.A. Gruber, Ritonavir-mediated induction of apoptosis in pancreatic cancer occurs via the RB/E2F-1 and AKT Pathways, Pharm. (Basel) 7 (1) (2014) 46–57.
[7] S. Dalva-Aydemir, R. Bajpai, M. Martinez, K.U. Adekola, I. Kandela, C. Wei, S. Singhal, J.E. Koblinski, N.S. Raje, S.T. Rosen, M. Shanmugam, Targeting the metabolic plasticity of multiple myeloma with FDA-approved ritonavir and metformin, Clin. Cancer Res 21 (5) (2015) 1161–1171.
[8] A. Srirangam, R. Mitra, M. Wang, J.C. Gorski, S. Badve, L. Baldridge, J. Hamilton, H. Kishimoto, J. Hawes, L. Li, C.M. Orschell, E.F. Srour, J.S. Blum, D. Donner, G. W. Sledge, H. Nakshatri, D.A. Potter, Effects of HIV protease inhibitor ritonavir on Akt-regulated cell proliferation in breast cancer, Clin. Cancer Res. 12 (6) (2006) 1883–1896.
[9] S. Kumar, C.S. Bryant, S. Chamala, A. Qazi, S. Seward, J. Pal, C.P. Steffes, D. W. Weaver, R. Morris, J.M. Malone, M.A. Shammas, M. Prasad, R.B. Batchu, Ritonavir blocks AKT signaling, activates apoptosis and inhibits migration and invasion in ovarian cancer cells, Mol. Cancer 8 (2009) 26.
[10] K.K. Ganta, B. Chaubey, Endoplasmic reticulum stress leads to mitochondria-mediated apoptosis in cells treated with anti-HIV protease inhibitor ritonavir, Cell Biol. Toxicol. 35 (3) (2019) 189–204.
[11] D.S. Zhong, X.H. Lu, B.S. Conklin, P.H. Lin, A.B. Lumsden, Q. Yao, C. Chen, HIV protease inhibitor ritonavir induces cytotoxicity of human endothelial cells, Arterioscler. Thromb. Vasc. Biol. 22 (10) (2002) 1560–1566.
[12] C. Austin, Observations on the penetration of the sperm into the mammalian egg, Aust. J. Biol. Sci. 4 (4) (1951) 581–596.
[13] C.R. Austin, The 'capacitation'of the mammalian sperm, Nature 170 (4321) (1952), 326-326.
[14] R.K. Naz, P.B. Rajesh, Role of tyrosine phosphorylation in sperm capacitation/acrosome reaction, Reprod. Biol. Endocrinol. 2 (1) (2004) 1–12.
[15] Y. Quan, Q. Liu, Effect of Akti-2 on sperm motility, capacitation and acrosome reaction in a mouse model, Biomed. Rep. 4 (5) (2016) 578–582.
[16] V. Sagare-Patil, M. Vernekar, M. Galvankar, D. Modi, Progesterone utilizes the PI3K-AKT pathway in human spermatozoa to regulate motility and hyperactivation but not acrosome reaction, Mol. Cell. Endocrinol. 374 (1–2) (2013) 82–91.
[17] J.-W. Bae, W.-S. Kwon, The deleterious toxic effects of bifenthrin on male fertility, Reprod. Toxicol. 101 (2021) 74–80.
[18] J.-W. Bae, W.-S. Kwon, Piperonyl butoxide, a synergist of pesticides can elicit male-mediated reproductive toxicity, Reprod. Toxicol. 100 (2021) 120–125.
[19] J.-W. Bae, S.-H. Kim, D.-H. Kim, J.J. Ha, J.K. Yi, S. Hwang, B.-Y. Ryu, M.-G. Pang, W.-S. Kwon, Ras-related proteins (Rab) are key proteins related to male fertility following a unique activation mechanism, Reprod. Biol. 19 (4) (2019) 356–362.
[20] C. Arend, M. Brandmann, R. Dringen, The antiretroviral protease inhibitor ritonavir accelerates glutathione export from cultured primary astrocytes, Neurochem. Res. 38 (4) (2013) 732–741.
[21] X. Lan, T. Kiyota, R. Hanamsagar, Y. Huang, S. Andrews, H. Peng, J.C. Zheng, S. Swindells, G.A. Carlson, T. Ikezu, The effect of HIV protease inhibitors on amyloid-β peptide degradation and synthesis in human cells and Alzheimer's disease animal model, J. Neuroimmune Pharmacol. 7 (2) (2012) 412–423.
[22] J.-M. Hwang, J.-W. Bae, E.-J. Jung, W.-J. Lee, W.-S. Kwon, Novaluron has detrimental effects on sperm functions, Int. J. Environ. Res. Public Health 19 (1) (2021) 61.
[23] R.K. Zeldin, R.A. Petruschke, Pharmacological and therapeutic properties of ritonavir-boosted protease inhibitor therapy in HIV-infected patients, J. Antimicrob. Chemother. 53 (1) (2004) 4–9.
[24] Food and Drug Administration, Fact sheet for healthcare providers: emergency use authorization for Paxlovid. 2021.
[25] World Health Organization, WHO model list of essential medicines 22nd list. 2021.
[26] B.D. Manning, L.C. Cantley, AKT/PKB signaling: navigating downstream, Cell 129 (7) (2007) 1261–1274.
[27] D.D. Sarbassov, D.A. Guertin, S.M. Ali, D.M. Sabatini, Phosphorylation and regulation of Akt/PKB by the rictor-mTOR complex, Science 307 (5712) (2005) 1098–1101.
[28] A.J. Koppers, L.A. Mitchell, P. Wang, M. Lin, R.J. Aitken, Phosphoinositide 3-kinase signalling pathway involvement in a truncated apoptotic cascade associated with motility loss and oxidative DNA damage in human spermatozoa, Biochem J. 436 (3) (2011) 687–698.
[29] H. Breitbart, T. Rotman, S. Rubinstein, N. Etkovitz, Role and regulation of PI3K in sperm capacitation and the acrosome reaction, Mol. Cell Endocrinol. 314 (2) (2010) 234–238.
[30] W.-J. Lee, E.-J. Jung, J.-M. Hwang, J.-W. Bae, W.-S. Kwon, GRP78 plays a key role in sperm function via the PI3K/PDK1/AKT pathway, Reprod. Toxicol. (2022).
[31] J.M. Gallardo Bolanos, C.M. Balao da Silva, P. Martin Munoz, A. Morillo Rodriguez, M. Plaza Davila, H. Rodriguez-Martinez, I.M. Aparicio, J.A. Tapia, C. Ortega Ferrusola, F.J. Pena, Phosphorylated AKT preserves stallion sperm viability and motility by inhibiting caspases 3 and 7, Reproduction 148 (2) (2014) 221–235.
[32] M.K. Jungnickel, K.A. Sutton, Y. Wang, H.M. Florman, Phosphoinositide-dependent pathways in mouse sperm are regulated by egg ZP3 and drive the acrosome reaction, Dev. Biol. 304 (1) (2007) 116–126.
[33] S. Zhang, M.J. Carper, X. Lei, W.T. Cade, K.E. Yarasheski, S. Ramanadham, Protease inhibitors used in the treatment of HIV+ induce β-cell apoptosis via the mitochondrial pathway and compromise insulin secretion, Am. J. Physiol. -Endocrinol. Metab. 296 (4) (2009) E925–E935.